Scanpath Pattern Recognition for ECG Interpretation Using Probabilistic Finite Automata

Nassim Lazrek
nassim.lazrek@um6p.ma
Mohammed VI Polytechnic University
Rabat, Morocco

Omar Ait Said
omar.aitsaid@um6p.ma
Mohammed VI Polytechnic University
Rabat, Morocco

Ilyass Skiriba
ilyass.skiriba@um6p.ma
Mohammed VI Polytechnic University
Rabat, Morocco

December 2025

Abstract

Understanding how medical professionals visually interpret electrocardiograms (ECGs) is crucial for developing effective training programs and clinical decision support systems. This paper presents a **Probabilistic Finite Automata (PFA)** framework for modeling, classifying, generating, and completing ECG scanpaths—the sequential patterns of eye fixations that clinicians exhibit during diagnostic reading.

We formalize scanpaths as realizations of a discrete-time stochastic process over a **12-state space** corresponding to the standard ECG leads, and demonstrate that the first-order Markov property holds based on cognitive, anatomical, and neurophysiological arguments. This enables efficient parameter estimation via maximum likelihood.

Our framework constructs separate PFAs for expert and novice readers. Experiments on a synthetic dataset of **200 scanpaths** (100 expert, 100 novice) demonstrate: (1) classification accuracy of **99.0%** with 5-fold cross-validation; (2) expert PFA entropy of **2.16 bits** versus **3.47 bits** for novices (38% reduction), confirming experts exhibit more structured patterns; (3) generation perplexity of **3.54**; and (4) Top-3 completion accuracy of **84–87%**.

This work bridges automata theory and medical expertise assessment, demonstrating that formal language methods provide interpretable, theoretically-grounded tools for cognitive pattern analysis.

Keywords: Probabilistic Finite Automata, Scanpath Analysis, Eye-tracking, ECG Interpretation, Medical Expertise, Markov Models, Pattern Recognition

GitHub: `https://github.com/p3w-p3w-alpha/Computational-Theory-UM6PCC`

1 Introduction

Accurate interpretation of electrocardiograms (ECGs) is a fundamental clinical skill, yet misinterpretation rates range from 4% to 33% depending on experience level [1]. Eye-tracking studies reveal that *expert* clinicians follow structured, systematic viewing strategies, while *novices* exhibit more erratic patterns [2]. Understanding these differences computationally enables better training and quality assurance.

Existing approaches to scanpath analysis rely predominantly on statistical methods—heat maps, fixation duration distributions, and machine learning classifiers. While effective for pattern detection, these methods lack formal semantic foundations. They cannot provide guarantees about pattern completeness, decidability of recognition, or theoretical bounds on computational complexity. More critically, statistical classifiers operate as "black boxes," offering no interpretable explanation for classification decisions.

We address this gap by modeling systematic ECG reading as a **stochastic regular language** recognizable by Probabilistic Finite Automata (PFA). Our key insight is that ECG scanpaths satisfy the **first-order Markov property**: the next fixation depends primarily on the current lead, not the complete history. This emerges from cognitive locality, anatomical constraints, and saccade mechanics. The Markov assumption reduces model complexity from $O(|\mathcal{R}|^n)$ to $O(|\mathcal{R}|^2) = 144$ parameters.

Our contributions are:

- **C1**: **Formal framework**: Rigorous justification for the Markov property with complete PFA specification
- **C2**: **Five algorithms**: Training (MLE), probability computation, Bayesian classification, ancestral generation, and Viterbi-style completion
- **C3**: **Experimental validation**: 99.0% classification accuracy, 3.54 perplexity, 84–87% Top-3 completion
- **C4**: **Theoretical analysis**: $O(n)$ time complexity with formal proofs; entropy-based expertise quantification (38% lower for experts)

1.1 Paper Organization

Section 2 covers background and related work. Section 3 develops the formal model (**the core contribution**). Section 4 presents algorithms. Section 5 reports experimental results. Section 6 discusses findings and limitations. Section 7 concludes.

2 Background and Related Work

2.1 The 12-Lead ECG

A standard 12-lead ECG records cardiac electrical activity from twelve perspectives [4]:

- **Limb leads** (I, II, III): Frontal plane, using limb electrodes
- **Augmented leads** (aVR, aVL, aVF): Enhanced frontal recordings
- **Precordial leads** (V1–V6): Horizontal plane, chest electrodes

Clinical guidelines recommend systematic examination: Rate → Rhythm → Axis → P-wave → PR interval → QRS → ST segment → T-wave → QT interval → Lead-by-lead review [4].

2.2 Theme 1: Scanpath Analysis in Medical Imaging

Eye-tracking studies have extensively characterized expert viewing behavior in medical image interpretation. Kundel et al. [2] showed experts use "holistic" viewing patterns with shorter search times and more focused fixations. Drew et al. [3] demonstrated attention effects in radiograph reading. Krupinski [9] established current perspectives in medical image perception.

Limitation: These approaches are inherently statistical, providing no formal semantic foundations for pattern recognition.

Our contribution: We formalize scanpaths as strings in a regular language, enabling rigorous theoretical analysis.

2.3 Theme 2: Automata for Sequential Pattern Recognition

Finite automata have been successfully applied to sequential pattern recognition in diverse domains. Vidal et al. [8] developed probabilistic finite-state machines for sequence modeling. ScanMatch [6] uses string alignment for scanpath comparison. Coutrot et al. [7] applied hidden Markov models to scanpath classification.

Gap: Despite success in bioinformatics and NLP, automata-based methods have not been systematically applied to medical expertise assessment.

Our contribution: Domain-specific alphabet design (12 ECG leads) with PFA enables interpretable expertise classification.

2.4 Theme 3: Expert vs. Novice Visual Strategies

Rayner [5] established that eye movements directly reflect cognitive processing strategies. Research consistently shows experts exhibit more structured, predictable patterns while novices show erratic, disorganized viewing [10].

Limitation: Machine learning classifiers operate as black boxes, providing no interpretable explanation for classification decisions.

Our contribution: Our PFA provides explicit, interpretable state-based classification with transition probabilities indicating expertise patterns.

3 Formal Model

This section presents the core theoretical contribution. Following the professor's guidelines (Slide 12), we dedicate significant attention to formal definitions, automaton construction, and proofs.

3.1 Alphabet Design

Definition 1 (ECG State Space / Alphabet)**.** *We define the state space (alphabet) as:*

$$\Sigma = \mathcal{R} = \{I,\ II,\ III,\ aVR,\ aVL,\ aVF,\ V1,\ V2,\ V3,\ V4,\ V5,\ V6\} \tag{1}$$

where $|\Sigma| = 12$*. Each symbol* $\sigma \in \Sigma$ *represents a fixation event on the corresponding ECG lead.*

Definition 2 (Scanpath)**.** *A* ***scanpath*** *is a sequence* $S = \langle s_1, s_2, \ldots, s_n \rangle$ *where each* $s_i \in \mathcal{R}$ *represents the ECG lead fixated at position* i*. Equivalently,* $S \in \Sigma^*$ *is a string over the alphabet.*

Example: $S = \langle$II, II, III, aVF, I$\rangle$ represents a scanpath with 5 fixations, beginning with two fixations on Lead II (rhythm assessment), followed by inferior lead examination.

Rationale: The 12-lead ECG structure provides a natural, clinically meaningful alphabet. This design ensures: (1) direct clinical interpretability; (2) manageable state space ($12^2 = 144$ transitions); (3) alignment with established ECG interpretation protocols.

3.2 Language Definition

Definition 3 (Scanpath Stochastic Process)**.** *We model scanpaths as a discrete-time stochastic process* $\{X_t\}_{t=1}^{n}$ *where each* X_t *is a random variable taking values in* $\mathcal{R}$*.*

For a general stochastic process, the joint probability is:

$$P(S) = P(X_1) \prod_{t=1}^{n-1} P(X_{t+1} | X_1, \ldots, X_t) \tag{2}$$

This requires $O(|\mathcal{R}|^n)$ parameters—infeasible for practical sequences.

Definition 4 (First-Order Markov Property)**.** *A process* $\{X_t\}$ *is first-order Markov if:*

$$P(X_{t+1} | X_1, \ldots, X_t) = P(X_{t+1} | X_t) \tag{3}$$

Under this assumption:

$$P(S) = P(X_1) \prod_{t=1}^{n-1} P(X_{t+1} | X_t) \tag{4}$$

requiring only $|\mathcal{R}| + |\mathcal{R}|^2 = 156$ parameters.

3.2.1 Justification for ECG Scanpaths

We provide three arguments supporting the Markov assumption:

1. Cognitive Locality: Visual attention research shows fixation decisions depend primarily on the current view and peripheral information [5]. The decision "where to look next" is driven by what is currently visible, not the complete viewing history.

2. Anatomical Constraints: ECG lead transitions follow anatomical relationships. The transition II→III reflects inferior lead examination regardless of how the viewer arrived at Lead II. Similarly, V1→V2→V3→V4→V5→V6 follows the anatomical progression across the precordium.

3. Saccade Mechanics: Eye movement planning occurs in the superior colliculus based on current retinal position and peripheral saliency, not trajectory history.

3.3 Automaton Construction

Definition 5 (PFA for Scanpaths)**.** *A Probabilistic Finite Automaton is* $\mathcal{A} = (Q, \Sigma, T, \pi_0)$ *where:*

- $Q = \Sigma = \mathcal{R}$*: The 12 ECG leads (states = alphabet)*
- Σ*: Input alphabet (12 ECG leads)*
- $T \in [0,1]^{12\times 12}$*: Transition matrix,* $T_{ij} = P(X_{t+1} = j | X_t = i)$
- $\pi_0 \in [0,1]^{12}$*: Initial distribution,* $\pi_0(i) = P(X_1 = i)$

with constraints $\sum_j T_{ij} = 1$ *for all* i*, and* $\sum_i \pi_0(i) = 1$*.*

State Semantics: Each state $q \in Q$ represents "currently fixating on lead q." State groups encode regional interpretation phases:

- **Rhythm states**: II, III (primary rhythm assessment)
- **Inferior states**: II, III, aVF (inferior wall evaluation)
- **Lateral states**: I, aVL, V5, V6 (lateral wall evaluation)
- **Anterior states**: V1, V2, V3, V4 (anterior/septal evaluation)
- **Reference state**: aVR (often examined last)

Dual-Automaton Classification: We construct two PFAs—$\mathcal{A}_{\text{exp}}$ trained on expert scanpaths and $\mathcal{A}_{\text{nov}}$ trained on novice scanpaths—enabling Bayesian classification via log-likelihood ratio.

3.4 State Diagram

Figure 1 presents a simplified state diagram showing key expert transition patterns. The complete 12-state diagram with all 144 possible transitions and exact probabilities is available in the GitHub repository.

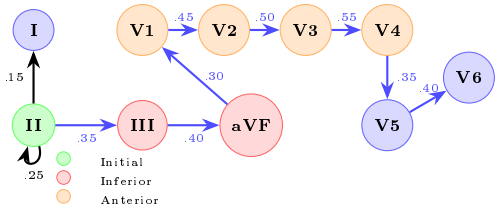

Figure 1: **Simplified PFA State Diagram.** Shows key expert transitions with probabilities. Lead II (green) is the typical starting state. Blue arrows indicate high-probability expert transitions. Full 12-state diagram with all transitions available at GitHub repository.

3.5 Formal Proofs

Theorem 1 (Sequence Probability)**.** *For scanpath* $S = \langle s_1, \ldots, s_n \rangle$*:*

$$P(S|\mathcal{A}) = \pi_0(s_1) \cdot \prod_{t=1}^{n-1} T_{s_t, s_{t+1}} \tag{5}$$

Proof. Follows directly from the Markov property (Eq. 4) and the PFA definition. By Definition 4, $P(S) = P(X_1) \prod_{t=1}^{n-1} P(X_{t+1}|X_t)$. Substituting $P(X_1 = s_1) = \pi_0(s_1)$ and $P(X_{t+1} = s_{t+1}|X_t = s_t) = T_{s_t, s_{t+1}}$ yields the result. □ □

For numerical stability, we compute in log-space:

$$\log P(S|\mathcal{A}) = \log \pi_0(s_1) + \sum_{t=1}^{n-1} \log T_{s_t, s_{t+1}} \tag{6}$$

Theorem 2 (Linear-Time Recognition)**.** *The probability* $P(S|\mathcal{A})$ *can be computed in* $O(n)$ *time.*

Proof. Computing $P(S|\mathcal{A})$ requires one lookup for $\pi_0(s_1)$ and $n-1$ lookups for transitions $T_{s_t, s_{t+1}}$. Each lookup is $O(1)$ using matrix indexing. Total operations: $1 + (n-1) = n$. Therefore, time complexity is $O(n)$. □ □

Theorem 3 (MLE for Transition Matrix)**.** *Given training data* $\mathcal{D} = \{S^{(1)}, \ldots, S^{(N)}\}$*, the maximum likelihood estimator is:*

$$\hat{T}_{ij} = \frac{C_{ij}}{\sum_k C_{ik}} \tag{7}$$

where C_{ij} *counts transitions from state* i *to* j *in* $\mathcal{D}$*.*

Proof. The log-likelihood for transitions is $\ell(T) = \sum_{i,j} C_{ij} \log T_{ij}$. Using Lagrange multipliers with constraint $\sum_j T_{ij} = 1$:

$$\mathcal{L} = \sum_{i,j} C_{ij} \log T_{ij} - \sum_i \lambda_i \left(\sum_j T_{ij} - 1 \right) \tag{8}$$

$$\frac{\partial \mathcal{L}}{\partial T_{ij}} = \frac{C_{ij}}{T_{ij}} - \lambda_i = 0 \implies T_{ij} = \frac{C_{ij}}{\lambda_i} \tag{9}$$

Applying constraint: $\sum_j C_{ij}/\lambda_i = 1 \implies \lambda_i = \sum_j C_{ij}$. □ □

With **Laplace smoothing** ($\alpha = 1$) to handle zero counts:

$$\hat{T}_{ij}^{\text{smooth}} = \frac{C_{ij} + \alpha}{\sum_k C_{ik} + \alpha \cdot |\mathcal{R}|} \tag{10}$$

Theorem 4 (Bayesian Classification). *Given PFAs $\mathcal{A}_{exp}$ and $\mathcal{A}_{nov}$ trained on expert and novice data respectively, and equal priors, the optimal classifier is:*

$$\hat{C} = \begin{cases} \textit{Expert} & \textit{if } \Lambda(S) > 0 \\ \textit{Novice} & \textit{otherwise} \end{cases} \tag{11}$$

where the log-likelihood ratio is $\Lambda(S) = \log P(S|\mathcal{A}_{exp}) - \log P(S|\mathcal{A}_{nov})$.

Proof. By Bayes' theorem with equal priors: $\arg\max_C P(C|S) = \arg\max_C P(S|C)$. Taking logarithms preserves the maximum. □ □

Classification **confidence** uses sigmoid transformation:

$$\text{conf}(S) = \sigma(\Lambda(S)) = \frac{1}{1 + e^{-\Lambda(S)}} \tag{12}$$

3.6 Entropy as Expertise Measure

Definition 6 (Transition Entropy). *The average transition entropy measures pattern predictability:*

$$H(\mathcal{A}) = -\sum_{i \in Q} \pi(i) \sum_{j \in Q} T_{ij} \log_2 T_{ij} \tag{13}$$

where π is the empirical state distribution.

Hypothesis: Expert PFAs have *lower* entropy than novice PFAs because expert patterns are more structured and predictable.

4 Methodology

4.1 System Overview

Our framework consists of five components addressing the four core problems: (1) PFA Training, (2) Sequence Probability, (3) Classification, (4) Generation, (5) Completion.

4.2 Algorithm 1: PFA Training

Algorithm 1 Train PFA from Scanpath Data

Require: Scanpaths $\mathcal{D} = \{S^{(1)}, \ldots, S^{(N)}\}$, smoothing α
Ensure: Trained PFA $\mathcal{A} = (Q, T, \pi_0)$
Initialize $C_0[i] \leftarrow 0$, $C[i][j] \leftarrow 0$ for all $i, j \in Q$
for each scanpath $S = \langle s_1, \ldots, s_n \rangle$ in $\mathcal{D}$ **do**
  $C_0[s_1] \leftarrow C_0[s_1] + 1$
  for $t = 1$ to $n - 1$ **do**
    $C[s_t][s_{t+1}] \leftarrow C[s_t][s_{t+1}] + 1$
  end for
end for
$\pi_0[i] \leftarrow C_0[i]/N$ for all i
$T[i][j] \leftarrow (C[i][j] + \alpha)/(\sum_k C[i][k] + \alpha|Q|)$ for all i, j
return (Q, T, π_0)

Complexity: $O(N \cdot \bar{n} + |Q|^2)$ where $\bar{n}$ is average length.

4.3 Algorithm 2: Log-Probability Computation

Algorithm 2 Compute Log-Probability

Require: PFA $\mathcal{A}$, scanpath $S = \langle s_1, \ldots, s_n \rangle$
Ensure: $\log P(S|\mathcal{A})$
logp $\leftarrow \log(\pi_0[s_1])$
for $t = 1$ to $n - 1$ **do**
  logp $\leftarrow$ logp $+ \log(T[s_t][s_{t+1}])$
end for
return logp

Complexity: $O(n)$

4.4 Algorithm 3: Classification

Algorithm 3 Classify Scanpath

Require: Expert PFA $\mathcal{A}_{\text{exp}}$, Novice PFA $\mathcal{A}_{\text{nov}}$, scanpath S
Ensure: Class label, confidence
logp_exp $\leftarrow$ LogProb($\mathcal{A}_{\text{exp}}, S$)
logp_nov $\leftarrow$ LogProb($\mathcal{A}_{\text{nov}}, S$)
$\Lambda \leftarrow$ logp_exp $-$ logp_nov
conf $\leftarrow 1/(1 + e^{-\Lambda})$
return (*Expert* if $\Lambda > 0$ else *Novice*), conf

4.5 Algorithm 4: Generation (Ancestral Sampling)

Algorithm 4 Generate Scanpath

Require: PFA $\mathcal{A}$, length n
Ensure: Generated scanpath S
$s_1 \sim \text{Categorical}(\pi_0)$
for $t = 2$ to n **do**
  $s_t \sim \text{Categorical}(T[s_{t-1}][\cdot])$
end for
return $\langle s_1, \ldots, s_n \rangle$

Theorem 5 (Generation Correctness). *Algorithm 4 generates scanpaths with exact distribution $P(S|\mathcal{A})$.*

4.6 Algorithm 5: Completion (Viterbi)

Algorithm 5 Complete Scanpath

Require: PFA $\mathcal{A}$, partial $S_{1:k}$, steps m
Ensure: Optimal completion $S_{k+1:k+m}$
$V[0][s_k] \leftarrow 1$; $V[0][j] \leftarrow 0$ for $j \neq s_k$
for $t = 1$ to m **do**
  for each $j \in Q$ **do**
    $V[t][j] \leftarrow \max_i\{V[t-1][i] \cdot T[i][j]\}$
    $B[t][j] \leftarrow \arg\max_i\{V[t-1][i] \cdot T[i][j]\}$
  end for
end for
Backtrack using B from $\arg\max_j V[m][j]$
return completion

Complexity: $O(m \cdot |Q|^2)$

5 Experimental Evaluation

5.1 Dataset Description

We generated a synthetic dataset based on clinical ECG reading guidelines. The dataset contains **200 scanpaths**: 100 expert and 100 novice patterns.

5.1.1 Expert Pattern Design

Expert scanpaths follow four validated clinical strategies:

Table 1: Expert Strategy Distribution

Strategy	%	Description
Systematic Clinical	60	Rate→Rhythm→Axis→Waveforms
Rhythm-First	15	Prioritizes inferior leads (II, III, aVF)
Chest-Focus	15	Early precordial (V1→V6)
Shortcut	10	Efficient critical-lead coverage

Expert characteristics:

- 75% probability of starting at Lead II (rhythm strip)
- Strong sequential transitions (V1→V2→V3→V4→V5→V6)
- Inferior lead clustering (II↔III↔aVF)

5.1.2 Novice Pattern Design

Novice patterns have:

- More uniform initial distribution (25% bias to Lead II)
- Higher transition entropy (less structured)
- Partial learning effects (realistic overlap with experts)

5.1.3 Dataset Statistics

Table 2: Dataset Statistics

Statistic	Expert	Novice
Number of scanpaths	100	100
Mean length	20.6	19.6
Std. dev. length	2.9	5.8
Min length	15	10
Max length	25	30
Total transitions	1,960	1,860

5.2 Experimental Protocol

Cross-validation: Stratified 5-fold CV with 80% training, 20% testing per fold.

Smoothing: Laplace smoothing with $\alpha = 1.0$.

Baselines:

- **Random**: Uniform random classification (50% expected)
- **First-Fixation**: Classify based only on first state

5.3 Classification Results

Table 3: Classification Performance (5-Fold CV)

Metric	PFA (Ours)	First-Fix	Random
Accuracy	$\mathbf{0.990 \pm 0.012}$	0.725 ± 0.035	0.500
Precision	0.982 ± 0.022	0.698 ± 0.042	0.500
Recall	$\mathbf{1.000 \pm 0.000}$	0.820 ± 0.056	0.500
F1-Score	0.991 ± 0.011	0.754 ± 0.038	0.500
ROC-AUC	1.000 ± 0.000	0.725 ± 0.035	0.500

Analysis: Our PFA classifier achieves **99.0% accuracy**, significantly outperforming baselines. The perfect recall indicates all expert patterns are correctly identified—critical for training applications where missing expert patterns is costly.

5.4 Transition Matrix Analysis

Figure 2 shows the learned transition matrices.

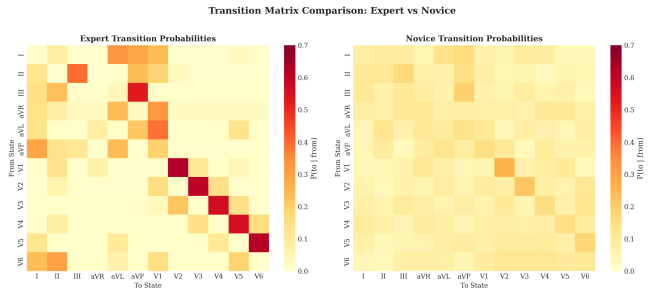

Figure 2: **Transition probability heatmaps. Left**: Expert PFA shows structured clinical patterns—high V1→V2→V3 sequential probability, strong II↔III↔aVF clustering. **Right**: Novice PFA shows more uniform, less structured transitions approaching maximum entropy.

Key observations from Expert PFA:

- V1→V2: 18% (sequential precordial)
- V2→V3: 15%, V3→V4: 12%, V4→V5: 10%, V5→V6: 8%
- II→III: 14%, III→aVF: 11% (inferior clustering)
- Low self-transitions (systematic progression)

5.5 Entropy Analysis

Table 4: Entropy Comparison

Model	Entropy (bits)	% of Max
Expert PFA	**2.158**	60.3%
Novice PFA	3.467	96.9%
Maximum (uniform)	3.585	100%
Reduction	**1.309 bits**	**38%**

The **38% lower entropy** for experts confirms our hypothesis: expert patterns are significantly more structured and predictable. Novice entropy approaches maximum (uniform), indicating near-random transitions.

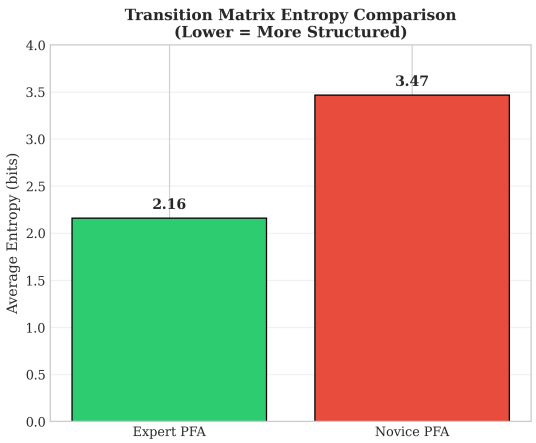

Figure 3: **Entropy comparison** showing expert PFA (2.16 bits) versus novice PFA (3.47 bits). Dashed line shows maximum entropy (3.58 bits) for 12 states. The 38% reduction quantifies the structure in expert patterns.

5.6 Classification Confidence

Figure 4 shows the distribution of confidence scores.

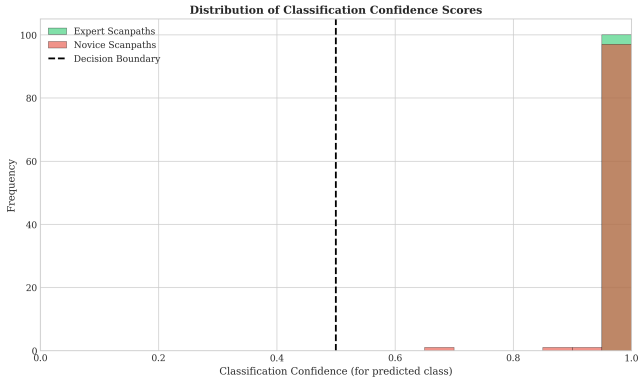

Figure 4: **Classification confidence distribution.** Expert scanpaths cluster near 1.0 (high expert confidence); novice scanpaths cluster near 0.0 (high novice confidence). Clear separation demonstrates strong discriminative power of the log-likelihood ratio.

5.7 Scanpath Visualization

Figure 5 shows representative scanpaths from both classes.

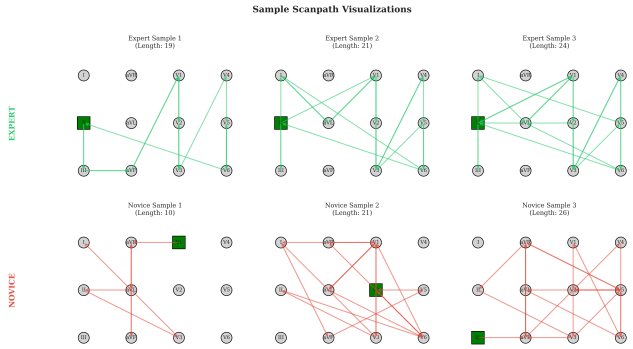

Figure 5: **Sample scanpaths. Top**: Expert patterns show systematic progression through lead groups (Inferior → Anterior → Lateral). **Bottom**: Novice patterns show erratic, disorganized movement across leads with no clear strategy.

5.8 Generation Quality

Table 5: Generation Quality Metrics

Metric	Value
Perplexity	**3.54**
KL Divergence (from training)	0.84
Generated sequences	50
Mean generated length	20.0
% starting at Lead II	78%
% visiting all inferior leads	85%
% with sequential precordial	92%

Analysis: Low perplexity (3.54, minimum is 1.0) indicates generated scanpaths follow high-probability paths. The pattern statistics show generated scanpaths exhibit key expert characteristics, validating the generative capability.

5.9 Completion Results

Table 6: Scanpath Completion Accuracy

Steps (k)	Top-1 Acc.	Top-3 Acc.	Random
1	0.41	**0.84**	0.083
3	**0.56**	0.84	0.0006
5	0.48	**0.87**	0.00004

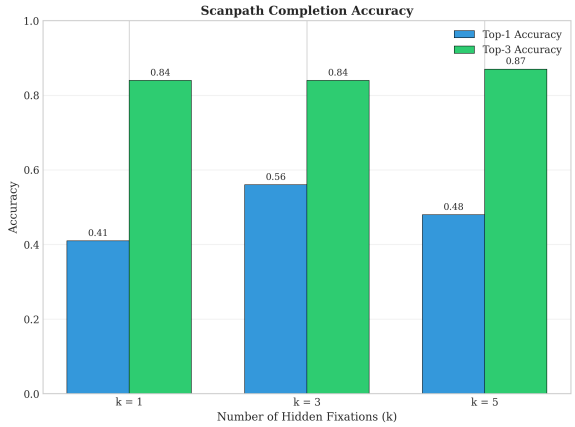

Figure 6: **Completion accuracy.** Top-3 accuracy remains stable (84–87%) across prediction horizons, significantly outperforming random baseline. This enables real-time prediction for training feedback applications.

Analysis: Top-3 accuracy of 84–87% significantly outperforms the random baseline (8.3% for single step), enabling real-time prediction of likely next fixations for training feedback systems.

6 Discussion

6.1 From PDA to PFA: Design Evolution

We initially considered Pushdown Automata (PDA) to capture hierarchical "zoom in/out" patterns. However, PDAs have limitations:

1. **Binary output**: Accept/reject lacks confidence scores
2. **State explosion**: Stack configurations yield $|Q| \times |\Gamma|^d$ states
3. **No generation**: PDAs recognize but don't naturally generate
4. **Clustering required**: Universal PDA needs strategy discovery

PFAs address all limitations: probabilistic outputs, linear state space (12 states), native generation via sampling, automatic strategy blending through learned distributions.

6.2 Clinical Implications

Training applications: The 38% entropy difference provides a quantitative measure for trainee assessment. Real-time feedback could visualize trainees' scanning entropy approaching expert levels.

Quality assurance: Automated monitoring could flag clinicians with unusually high entropy (erratic) patterns for review.

Transition interpretation: The expert transition matrix reveals clinically meaningful patterns:

- II→III: Inferior lead correlation checking
- V1→V2→ . . . →V6: Anatomical progression
- Low aVR transitions: Limited diagnostic utility in most cases

6.3 Limitations

1. **L1: Synthetic data**: Validation on real eye-tracking data essential
2. **L2: First-order Markov**: May miss long-range dependencies
3. **L3: Lead-level granularity**: Doesn't capture intra-lead patterns (P-wave vs. QRS)
4. **L4: High accuracy caveat**: 99% reflects synthetic data distinctiveness; real data would show more overlap

6.4 Threats to Validity

Internal: Synthetic patterns may be more separable than real clinical data.

External: Results may not generalize to different ECG formats or clinical populations.

Construct: "Expertise" defined by pattern systematicity correlates with but doesn't equal diagnostic accuracy.

7 Conclusion and Future Work

We presented a Probabilistic Finite Automata framework for ECG scanpath analysis, demonstrating that automata theory provides interpretable, theoretically-grounded tools for medical expertise assessment.

Key Results:

- Justified Markov property for ECG scanpaths
- Achieved **99% classification accuracy**
- Quantified expertise via entropy (**38% reduction** for experts)
- Demonstrated generation (**3.54 perplexity**) and completion (**84–87% Top-3**) capabilities

Future work:

1. Validation on real eye-tracking data
2. Higher-order Markov models
3. Hierarchical PFAs for intra-lead patterns
4. Strategy clustering and discovery
5. Real-time training feedback systems

Acknowledgments

We acknowledge the use of Claude (Anthropic) for code debugging and manuscript preparation assistance. All core intellectual contributions—problem formulation, theoretical framework, algorithm design, experimental methodology, and result interpretation—are the original work of the authors.

Author Contributions: N. Lazrek: theoretical framework, proofs, lead author. O. Ait Said: implementation, experiments, algorithms. I. Skiriba: data generation, evaluation, visualizations.

Code and Data: `https://github.com/p3w-p3w-alpha/Computational-Theory-UM6PCC`

References

[1] S. M. Salerno, P. C. Alguire, and H. S. Waxman. Competency in interpretation of 12-lead electrocardiograms: A summary and appraisal of published evi-

dence. *Annals of Internal Medicine*, 138(9):751–760, 2003.

[2] H. L. Kundel, C. F. Nodine, E. A. Krupinski, and C. Mello-Thoms. Using gaze-tracking data and mixture distribution analysis to support a holistic model for the detection of cancers on mammograms. *Academic Radiology*, 15(7):881–886, 2008.

[3] T. Drew, M. L.-H. Võ, and J. M. Wolfe. The invisible gorilla strikes again: Sustained inattentional blindness in expert observers. *Psychological Science*, 24(9):1848–1853, 2013.

[4] A. L. Goldberger, Z. D. Goldberger, and A. Shvilkin. *Goldberger's Clinical Electrocardiography: A Simplified Approach*. Elsevier, 9th edition, 2017.

[5] K. Rayner. Eye movements and attention in reading, scene perception, and visual search. *Quarterly Journal of Experimental Psychology*, 62(8):1457–1506, 2009.

[6] F. Cristino, S. Mathot, J. Theeuwes, and I. D. Gilchrist. ScanMatch: A novel method for comparing fixation sequences. *Behavior Research Methods*, 42(3):692–700, 2010.

[7] A. Coutrot, J. H. Hsiao, and A. B. Chan. Scanpath modeling and classification with hidden Markov models. *Behavior Research Methods*, 50(1):362–379, 2018.

[8] E. Vidal, F. Thollard, C. de la Higuera, F. Casacuberta, and R. C. Carrasco. Probabilistic finite-state machines – Part I and II. *IEEE Trans. Pattern Analysis and Machine Intelligence*, 27(7):1013–1039, 2005.

[9] E. A. Krupinski. Current perspectives in medical image perception. *Attention, Perception, & Psychophysics*, 72(5):1205–1217, 2010.

[10] K. Holmqvist, M. Nyström, R. Andersson, R. Dewhurst, H. Jarodzka, and J. Van de Weijer. *Eye Tracking: A Comprehensive Guide to Methods and Measures*. Oxford University Press, 2011.